Case Studies in Thermal Engineering 53 (2024) 103914

Contents lists available at ScienceDirect

Case Studies in Thermal Engineering

journal homepage: www.elsevier.com/locate/csite

A handy model for the dynamic thermal response of the building-plant system

Carmela Concilio [b], Pasquale Cucco [b], Giacomo Di Ruocco [b], Gennaro Cuccurullo [a,*]

[a] Department of Industrial Engineering University of Salerno, Via Giovanni Paolo II, 84084, Fisciano, Italy
[b] Department of Civil Engineering University of Salerno, Via Giovanni Paolo II, 84084, Fisciano, Italy

ARTICLE INFO

Handling Editor: Huihe Qiu

Keywords:
Building thermal comfort
Energy consumption
Building HVAC control
Predictive
Functional control
Energy saving in building

ABSTRACT

This paper presents a novel approach for predicting the unsteady indoor room temperature as resulting from the interrelation among the characteristics of the thermal plant, the temperature regulation system, and the envelope, allowing an easy-to-handle but meaningful description. A finite element model is built by dividing the analysis domain into two separate sub-systems suitably coupled. The former represents the 1D unsteady composite wall, the latter describes the inner ambient regarded as a lumped thermal system. The development of optimal thermal regulation strategies in terms of comfort and energy savings is made easier. Simulation results revealed that a good level of comfort can be ensured by adopting different thermal regulation strategies for 'light' and 'massive' envelopes.

1. Introduction

In the first half of the last century, as long as it was of interest to estimate heat losses and to size winter installations in buildings with heavy walls and small openings, it was appropriate to adopt stationary conditions, cancelling the role of the thermal capacity of the walls, [1]. The steady-state room heat transfer corresponding to worst outside weather conditions defined the design conditions (hereinafter referred to with the superscript "*"). The framework changed in the middle of the 20th century: light buildings provided less capacity and their larger glazed areas allowed large solar gains. By introducing the dynamic description in heat transfer modelling, certain phenomena well-known from experience may be considered, [2]. For instance, it is generally known from experience that thick, massive walls, are less affected by short-term variations in ambient temperature than are thin walls. Therefore, a dynamic description of the building-wall thermal response was required. A first approach consists in solving the Fourier Continuity Equation in One Dimension for multilayered walls with distributed resistance and capacity: often this task is done conventionally with a simple sinusoidal description of the outer temperature, see the comprehensive work by Davies [3–6]. In this connection, the European regulation UNI EN ISO 13786 returns the thermal response of multi-layered walls assuming that the temperature of the internal environment does not change in relation to the nominal value. This behaviour may be related to an infinite thermal capacity of the internal environment or to an ideal thermal plant, able to instantly balance thermal loads. This is a straightforward matter to deal with, it involves the introduction of the periodic transmittance to describe the heat flux at inner surface as the result of the sinusoidal excitation at the external surface, [1]. In order to allow a more accurate description involving the interrelated behaviour among the involved sub-systems (namely: building walls, HVAC plants and the supporting temperature regulation systems, external climate and inner sources), a broad class of software that relies on numerical processing for simulating the unsteady thermal performance of

* Corresponding author.
E-mail address: gcuccurullo@unisa.it (G. Cuccurullo).

https://doi.org/10.1016/j.csite.2023.103914
Received 8 May 2023; Received in revised form 27 July 2023; Accepted 11 December 2023
Available online 17 December 2023

buildings has been well established for many decades. There are a number of relevant examples: DOE, TRNSYS, BLAST, EnergyPlus, Genopt, MatLab/Simulink, SUNCODE, COMSOL, [7–10]. In this category, an interesting work was proposed in Ref. [11] where a sophisticated multi-objective algorithm interacting with EnergyPlus was implemented in Python code.

A great deal of self-produced software applications for dynamically simulating the interaction between plants and buildings can be found, e.g. Refs. [12–18]. As regards this typology, many studies can be found which are based on the MATLAB/Simulink environment to simulate heating plants in terms of temperature control and efficiency, [19–26]. They give surprisingly realistic information on the operation of actual control systems, both in combination with other plants and for different types of buildings, showing the effect of different control strategies. A novel class of papers uses a dynamic model of the process or artificial neural network trained on-site using local indoor measurements in order to anticipate the future behavior of the system and optimize the future response of a plant [27–31]. In any case, detailed simulation may involve the need to purchase and learn commercial software that requires resources and time costs. In answer to those limitations, a FEM model coupling the 1D unsteady composite wall with a lumped thermal system for the inner ambient is proposed. The objective is to look in an integrated way at the thermal response of the environment, the heating plant and the building-wall, allowing for a simplified yet meaningful description. In what follows, two case studies are considered as an application of the present model. The buildings under study are emblematic examples of modern production southern Italy, [32,33].

2. Tools and methods

The analysis of the "building-plant system" is related to the integrated coexistence of two subsystems, Fig. 1: {1} the inner environment, described as a lumped body, is separated from the outdoor ambient by a one-dimensional multi-layered wall {2}, described as a body with distributed parameters. The thermal plant {3} operating in the internal environment consists of a fancoil driven by a thermostatic or climate control; it is supposed with negligible inertia.

Numerical simulations were carried out by the finite element method on COMSOL Multiphysics. The multilayered 1D-wall was coupled to a 0D Lumped Thermal System model. Boundary conditions of III kind on both sides were assumed for the building-wall. The outdoor temperature was considered as a known function, depending on the local weather conditions, while the indoor temperature determined the coupling of the wall to the inner ambient. By analogy with electrical circuits, the FEM code provides a lumped element model that idealizes the domain and boundary conditions for heat transfer into components which, for the present case, turn out to be one convective thermal resistance and one thermal mass, see next paragraph. At this point, the convergence of the numerical solution was verified by checking the effect of changes in mesh sizing, and the numerical solution was compared to a closed-form solution based on the limiting case of infinite-capacity inner ambient.

2.1. The multi-layered wall

The wall consists of layers of material with distributed resistance and capacity where the unsteady heat transfer is due to pure conduction. The transient state equation of heat conduction for each layer featuring the 1D geometry is

$$\rho c \frac{\partial T}{\partial t} = \nabla \cdot (k \nabla T) \quad [1]$$

where ρ is the density, c the heat capacity, k the thermal conductivity, T the temperature.

Third kind boundary conditions are prescribed on both the exposed surfaces:

$$\underline{\mathrm{n}} \cdot \underline{\dot{\mathrm{q}}} = h \left(T_{\mathrm{wall}}(t) - T_{\mathrm{ext.\ surroundings}}(t) \right) \quad [2]$$

where conduction heat transfer balances convective heat transfer at wall. The heat transfer coefficients are given on both boundaries. Therefore, the problem turns out to be linear.

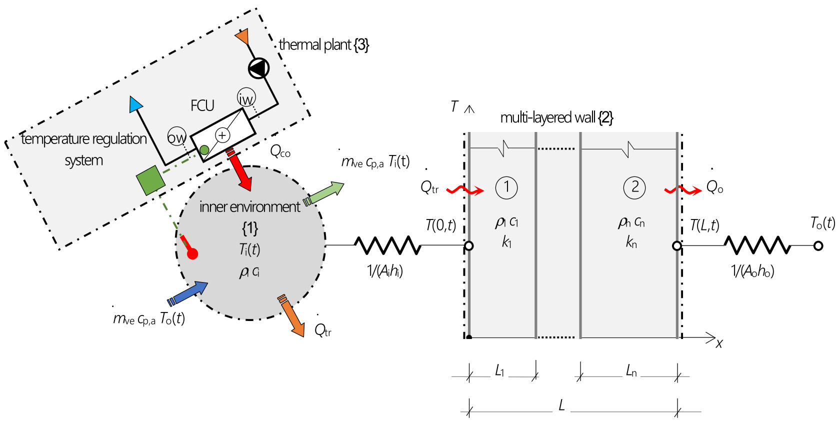

Fig. 1. Sketch of the problem.

2.2. The fancoil unit

The indoor heating unit is supposed to be a fancoil (FCU), i.e. a water-to-air heat exchanger; therefore, the heating capacity delivered by the water (hot fluid, subscript “w”) to the inner air (cold fluid, subscript "i") can be cast in the form [8,34,35],

$$\dot{Q}_{\mathrm{co}} = U[T_{\mathrm{wi}}(t) - T_i(t)] \quad [3]$$

where the subscript "wi" refers to the water inlet, the specific-heating-capacity U refers to the heating capacity delivered by the FCU as driven by unitary maximum temperature difference over the device. The expression holds if the changes in temperature from the design conditions are moderate. The use of this parameter is convenient for rating the performance of the FCU because it turns out to depend exclusively on air and water mass flow rates. Therefore, considering design conditions, the term $U^* = \dot{Q}^*_{\mathrm{co}}/[T^*_{\mathrm{wi}} - T^*_i]$ can be easily evaluated after the knowledge of the exchanger inlet parameters alone. The latter are known for the rating problem at hand.

2.3. The inner environment

The indoor ambient is described as a lumped thermal system. This approach allows a simplified handling of the model meanwhile retaining the essential features of the inner ambient: the inner ambient is envisioned like a sub-system made of a thermal mass, heat capacity C_{i}, thermally coupled to the building envelope by the internal thermal convective resistance R_{hi}. The thermal mass is subjected to diffusive heat loads through the wall, $\dot{Q}_{\mathrm{tr}}$, and ventilation loads, $\dot{Q}_{\mathrm{ve}}$, while it is heated by a fancoil unit ($\dot{Q}_{\mathrm{co}}$). Therefore, the inner-ambient energy balance equation turns out to be, Fig. 1:

$$C_i \frac{\partial T_i}{\partial t} = \dot{Q}_{\mathrm{co}} - \dot{Q}_{\mathrm{tr}} - \dot{Q}_{\mathrm{ve}} \quad [4]$$

The instantaneous heat leaving the inner ambient is expressed with reference to the convective heat flow at the inner surface:

$$\dot{Q}_{\mathrm{tr}} = [T_{\mathrm{i}}(t) - T_1(0,t)] / R_{\mathrm{hi}} \quad [5]$$

where "1" indicates the first layer of the wall and $R_{\mathrm{hi}} = (h_{\mathrm{i}}A)^{-1}$ is the inner resistance, A being the wall heat transfer surface area.

The ventilation term is due to an external air mass flow, $\dot{m}_{\mathrm{ve}}$:

$$\dot{Q}_{\mathrm{ve}} = \dot{m}_{\mathrm{ve}} c_{\mathrm{p,air}} [T_i(t) - T_o(t)] \quad [6]$$

3. Case studies

In Italy, there is a modern building heritage that has peculiar and emblematic features typical of post-war reconstruction (World War II). It is evidence of an entire country’s desire for sociocultural recovery. The construction techniques of this period highlight the transition from a predominantly ‘massive’ envelope, with a mixed masonry-concrete structure, to one of a ‘light’ type, with a reinforced concrete framed structure and light infills. In this connection, two representative examples of modern architecture in the city of Salerno, Italy, were considered. They are evidence of two different building systems that characterized the urban development of Salerno in the 19th century, both in terms of architectural and constructional features:

- wall-1: district Bruno Zevi (1958–62), with reinforced concrete framed structure and external face brick facade; the envelope is of the lightweight, double-wall type, with air space in between. The facade communicating with the interior rooms is plastered. Table 1 lists the related properties (thickness, L, thermal conductivity, k, density, ρ, specific heat, c).
- wall-2: The House of Mutilate (1956), with a mixed structure (reinforced concrete/masonry) and plaster exterior face; the shell is of the massive type, in yellow Neapolitan tuff, collaborating with the load-bearing structure. Both facades, inner and outer, are plastered. See Table 2 for the related properties.

Tables 3 and 4 result from processing the geometric and thermophysical data inherent to the two walls. The Tables below show that wall-1 is preferable to wall-2 from a stationary point of view, the static transmittance U_{st} being lower for wall-1. On the other hand, wall-2 has a better thermal behavior than wall-1 from a dynamic point of view, the periodic thermal transmittance U_{dyn} being lower for wall-2. In quantitative terms, according to the EN ISO 13786 standard, the attenuation factor, f, and the delay time, φ, are invoked as performance indexes to classify the behavior of the wall: wall-1 falls in the second band for thermal quality, whereas wall-2 falls in the first one.

The inner ambient is featured as follows: plan dimensions are of 15 × 10 m, its height is of 3 m, the frontal area of surfaces exposed to the external environment is 25 m^2, furniture correspond to 600 kg of wood (ρ = 450 kg/m^3, c = 1380 J/(kg K)).

Table 1
Wall-1: geometrical and thermal properties.

layer	L [m]	k [W m^{-1} K^{-1}]	ρ [kg m^{-3}]	c [J kg^{-1} K^{-1}]
1	0,02	0,700	1400	830
2	0,1	0,360	1000	1000
3	0,04	0,0250	1,22	1005
4	0,12	0,720	1800	1000

Table 2
Wall-2: geometrical and thermal properties.

layer	L [m]	k [W m^{-1} K^{-1}]	ρ [kg m^{-3}]	c [J kg^{-1} K^{-1}]
1	0,02	0,7	1400	830
2	0,44	0,63	1500	1300
3	0,02	0,9	1800	840

Table 3
– Wall-1: static and dynamic featuring.

U_{st} [Wm^{-2} K^{-1}]	U_{dyn} [Wm^{-2} K^{-1}]	f	φ [h]
0.45	0.123	0.273	10.35

Table 4
Wall-2: static and dynamic featuring.

U_{st} [Wm^{-2} K^{-1}]	U_{dyn} [Wm^{-2} K^{-1}]	f	φ [h]
1.088	0.049	0.045	18.43

Outer and inner thermal boundary conditions are featured by specifying the following values for the heat transfer coefficients: $h_o = 25$ W/(m^2 K) and $h_i = 7.69$ W/(m^2 K); the initial temperature is assumed to match the indoor target temperature, $T_i{*} = 20$ °C, while the outer design temperature is $T_o{*} = -5$ °C.

Natural ventilation is supposed to realize a fresh air flow equal to a half of room's total space in an hour, [36].

The nominal size of the FCU is supposed such as to meet the design ambient load ($\dot{Q}^*_{co,wall\text{-}1} = 2130$ W, $\dot{Q}^*_{co,wall\text{-}2} = 2520$ W) at the average fan speed. Thus, assuming inlet temperatures equal to $T_{wi}{*} = 50$ °C and $T_i{*} = 20$ °C for water and air respectively, it follows that the specific heating capacities turn out to be $U_{ave,wall\text{-}1} = 71$ W/K and $U_{ave,wall\text{-}2} = 84$ W/K. Considering that the water flow through the fancoil does not vary, these values change only as the fan speed changes. It is assumed that a fan speed greater than the design speed is available, that leading to increased specific heating capacities. According to the typical relationship $U_{max} = U_{ave}/\ 0.85$, one has $U_{max,wall\text{-}1} = 83$ W/K and $U_{max,wall\text{-}2} = 99$ W/K.

At this point, the model at hand was aimed at predicting the indoor ambient temperature as resulting from the interrelation between the thermal plant features and the two types of envelopes at hand, with completely different technological characteristics and thermohygrometric behaviors. In turn, the availability of the internal temperature allows to evaluate energy consumptions in relation to both the thermal regulation strategy in use and the performance of the FCU.

4. Results and discussion

4.1. Model validation

Firstly, the model was validated against the UNI EN 13786 predictions for the wall featured in Table 5. For this purpose, the indoor environment was considered as a thermal reservoir with a constant and uniform temperature (infinite capacity ambient) fixed to the initial value, equal to the design inner temperature. Meanwhile, a sinusoidal outdoor temperature variation is imposed until periodic steady state conditions are recovered. The relative error turned out to be 3.3 % and 3.4 % in terms of periodic thermal transmittance and time lag, respectively. Moreover, an approximate analytical solution for the problem at hand derived within the framework of weighted residuals, see Ref. [8] for a complete description, was compared with results arising from the present model. In this case, the ability of the model at hand to follow-up the dynamic behaviour of the system at hand seems clear. Satisfactory results were obtained, see Table 6 reporting the maximum relative error within the wall.

4.2. Definition of the time frames

The model at hand is employed to enlighten the thermal response of two different meaningful architecture systems in Campania, Italy. To mitigate the effect of arbitrary fixed initial conditions, the two walls have been subjected to a fictitious sinusoidal forcing with a 24-h period. Indeed, it has been considered that the level and amplitude in use as well as high frequency fluctuations have no impact on the objective pursued. The initial temperature was arbitrarily set to 20 °C, uniform on the entire wall. At this point, the purpose of

Table 5
Building Wall structure.

LAYER	k [W m^{-1} K^{-1}]	ρ [kg m^{-3}]	c [J kg^{-1} K^{-1}]	L [cm]
Brick 1	0.777	1800	920	8
Polyurethane	0.045	335	850	5
Brick 2	0.400	1800	920	14

Table 6
Maximum relative error.

time [h]	Max [%]
6	1.28
12	1.24
18	0.66
24	1.60

the investigation was to ascertain how long it would take to reduce in a tangible way the effects of the initial condition. To detect such an occurrence, the current temperature of the interior surface averaged over 24-h period is chosen to mark the attainment of stabilized periodic conditions. Then, the extinction time is defined so that the mean internal temperature does not exceed 5 % of the corresponding asymptotic value. According to this criterion, the extinction time for wall 2 (103.2 h) is about 3 times the one for wall 1 (46.4 h), see Fig. 2. It should be noted that the phase shift of walls according to the EN 13786 Standard is a measure of the extinction time; however, the latter is calculated by looking for a realistic estimate of the time it takes to process local external temperatures after reaching near stable conditions. Moreover, since the extinction time is based on the trend of the inner wall temperature, its choice seems suitable in view of its significance for both the well-being of the occupants and the instantaneous ambient heat loads.

Next, processing of meteorological conditions in Salerno in the winter of 2021, allowed to identify a timeframe going from 24 to 29 January where an almost homogeneous daily temperature tendency occurs, see Fig. 3. As a result, for both structures under review, the analysis is limited to the 24 h following the larger of the two extinction times, starting from 7 a.m. 28 January. The latter is the same approach on which is based the standard UNI 5664 for the acceptance tests of heating plants.

4.3. Thermal regulation strategies

Two alternative criteria are adopted to adjust the fancoil delivered heating power because of perturbations on design conditions which here are supposed to be due to changes in outdoor temperature alone.

4.3.1. Thermostatic temperature control

The former indoor temperature control strategy (TSR) foresees an ON/OFF method for the FCU control valve (either two or three-way) driven by the actual indoor temperature itself. It is a basic closed-chain control, suitable for the application under consideration. In practice, depending on the state of the FCU control-valve, which can be either fully closed or fully open, the delivered heating power is supposed to be zero or non-zero.

Since a temperature difference of 1 °C around the target value is fixed for TSR, the internal air temperature fluctuates in the prescribed band for the two walls at hand, since no overshoots are encompassed in the current model. The resulting average values are not significantly different from the target, Fig. 4. Since the average indoor temperature is virtually unchanged, the computed consumption remains essentially independently of the FCU fan speed in use, turning out to be 27 kWh for wall-1 and 30 kWh for wall-2. In all cases, the cycle-frequency decreases next to the warmest hours, in accordance with the delay associated with the inertia of the walls.

Not surprisingly, with increasing the FCU fan speed, the number of switching cycles increases. In fact, reaching the maximum temperature-band level occurs in a shorter time while the decay time toward the lower band level remains unchanged.

It is interesting to note that lower static transmittance promotes the reduction of the cycle-frequency, whereas thermal inertia exhibits an opposite tendency. Because the dynamic features of wall-2 are better that wall-1, this occurrence compensates for its weaker static features and explains why a similar number of cycles affects both walls, [34].

4.3.2. Climatic temperature control

The latter temperature control strategy fixes the water supply temperature to the FCU as a function of the external one (CLR), according to the linear relationship:

$$T_{w,i}(t) = \frac{T_i^* - T_{w,i}^*}{T_{off} - T_o^*}\left(T_o(t) - T_o^*\right) + T_{w,i}^* \qquad [7]$$

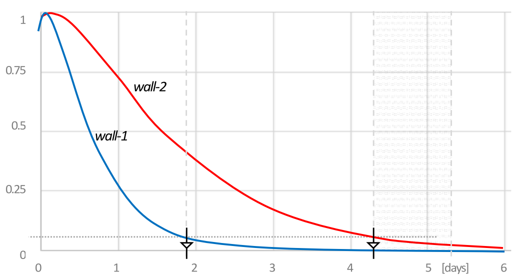

Fig. 2. Initial condition's extinction time.

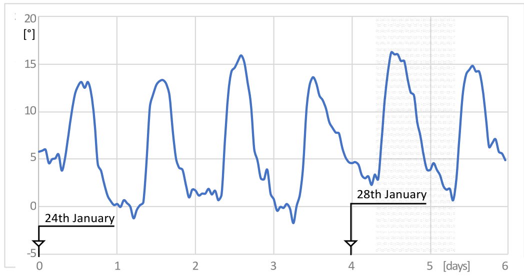

Fig. 3. Outside temperature evolution in Salerno from 24th gen 2021.

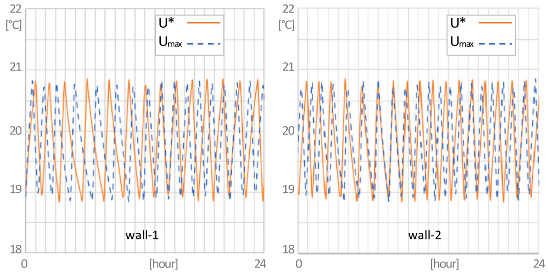

Fig. 4. TSR.

where T_{off} specifies the heating plants shutdown temperature; it is an open loop control whose accuracy depends on how suitable the algorithm given by eq. (3) turns out to be. The FCU water inlet temperature is adjusted by assuming the following parameters: $T_o* = -5$ °C, $T_{off} = 20$ °C. It should be noted that the choice of the T_{off}-value is related to the supposed absence of internal loads.

CLR is successful in guaranteeing the inner temperature to be close to the target value for both walls when the average fan speeds are in use, the corresponding values being 19.9 and 20.4 °C for wall-1 and wall-2, with mean deviation of 0.31 and 0.71 °C for wall-1 and wall-2, respectively (see Fig. 5). These rather satisfactory results concerning the capacity of the control algorithm come from the assumption of no interference due to internal loads and from the achievement of stable conditions. This also suggest that the lighter wall is better regulated than the other wall when using the CLS: indeed, the thermal control algorithm does not consider the delay between the external and internal temperature peaks caused by the inertia of the walls. The correctness of the adopted linear relationship should be improved.

When average fan speed is in use, only small differences from the case analysed in the previous paragraph result from the calculations, the energy loss being 27.2 and 31 kWh for wall-1 and wall-2, respectively. When the FCU runs at the higher speed, as expected, the internal temperature values are higher than those associated with the design speed, turning out to be 21.1 and 21.5 °C. In consequence, energy losses turn out to be 30 and 34 kWh, respectively.

5. Conclusions

A simple and easy-to-handle, yet accurate, thermal model to evaluate the dynamic thermal response of the building-plant system was developed. The model allows to study the wall envelope performance encompassing the ability to account for the influence of the internal environment and of the plant feature, as well. The effect of the indoor features is ignored by the standard EN ISO 13786 and usually requires the involvement of specific software and algorithms that are more cumbersome and expensive to purchase. Two emblematic examples of modern architecture in the south of Italy have been studied as an example of application, that bringing to light important quantitative differences.

Further developments of the present work are intended to include inertial effects of the thermal plant and the introduction of the heat pump performances, while more sophisticated temperature regulation strategies are to be involved to optimize energy consumptions.

Author statement

With the submission of this manuscript I would like to undertake that:

- All authors of this Article have directly participated in the planning, execution, or analysis of this study;
- All authors of this paper have read and approved the final version submitted;

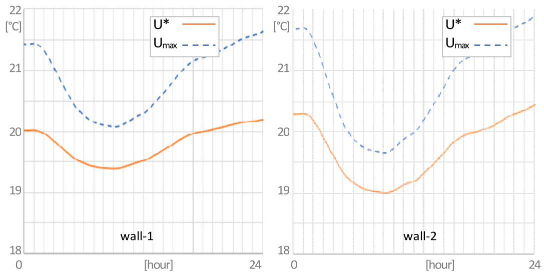

Fig. 5. CLR.

- The contents of this manuscript have not been copyrighted or published previously;
- The contents of this manuscript are not now under consideration for publication elsewhere, while acceptance by the Journal is under consideration;

We have no conflicts of interest to disclose.

Declaration of competing interest

We have no conflicts of interest to disclose.

Data availability

No data was used for the research described in the article.

References

[1] M.G. Davies, Building Heat Transfer, Wiley, 2004, 2004, ISBN 9780470020548.
[2] C.A. Balaras, The role of thermal mass on the cooling load of buildings, An overview of computational methods,Energy and Buildings 24 (Issue 1) (1996) 1–10. ISSN 0378-7788.
[3] M.G. Davies, Optimum design of resistance and capacitance elements in modelling a sinusoidally excited building wall, Build. Environ. 18 (1–2) (1983) 19–37. ISSN 0360-1323.
[4] M.G. Davies, The thermal response of an enclosure to periodic excitation: the CIBSE approach, Build. Environ. 29 (2) (1994) 217–235. ISSN 0360-1323.
[5] M.G. Davies, Solutions to Fourier's equation and unsteady heat flow through structures, Build. Environ. 30 (3) (1995) 309–321. ISSN 0360-1323.
[6] M.G. Davies, A time-domain estimation of wall conduction transfer function coefficients, Build. Eng. 102 (1996) 401, parte 1, 328–343. 397.
[7] J. Savoyat, Kevyn Johannes, Joseph Virgone, Integration of thick wall in trnsys simulation, 30th ISES Biennial Solar World Congress 2011, SWC 2011 3 (2011) 1836–1847.
[8] C. Concilio, P. Di Luccia, G. Cuccurullo, An approximate analytical solution for dynamic heat transfer of building walls, Case Studies in Thermal Engineering, Case Stud. Therm. Eng. 42 (102693) (2023). ISSN 2214-157X.
[9] A. Mahdavi, C. Pröglhöf, A model-based method for the integration of natural ventilation in indoor climate systems operation, in: Building Simulation, 2005, pp. 685–692.
[10] Ioannis Alexopoulos, Christos Tzivanidis, Evangelos Bellos, Georgios Mitsopoulos, Dimitrios Korres, Thermal Behavior of a Building Simulation Using COMSOL, 201, Conference: 7th IC-SCCE At: Athens, Vol: vol. 2, pp.409-413.
[11] O. Nassima, L. Hocine, B. Youcef, A. Abdelyazid, Indoor temperature regulation and energy consumption inside a working office in building system using a predictive functional control, Energy Sources, Part A Recovery, Util. Environ. Eff. (2021), https://doi.org/10.1080/15567036.2021.2017517.
[12] G. Hudson, C.P. Underwood, A simple building modelling procedure for MATLAB/SIMULINK, in: 6a Conferenza Internazionale IBPSA, 1999, pp. 777–783. Kyoto, Giappone.
[13] E. Nannei, C. Schenone, Thermal transients in buildings: development and validation of a numerical model, Energy Build. 29 (3) (1999) 209–215.
[14] N. Mendes, G.H. Oliveira, H.X. de Araújo, Building Thermal Performance Analysis by Using Matlab/simulink, Seventh International IBPSA Conference, Rio de Janeiro, Brazil, 2001, August, pp. 473–480.
[15] D.G. Stephenson, G.P. Mitalas, Calculation of heat conduction transfer functions for multilayer slabs ASHRAE Transactions 77 (2) (1971) 117–126.
[16] L. Yan, Y. Liu, Z. Wuxing, L. Tang, Z. Xiangrong, L. Jiaping, A novel building energy efficiency evaluation index: establishment of calculation model and application, Energy Convers. Manag. 166 (2018) 522–533. ISSN 0196-8904.
[17] K.A. Antonopoulos, C. Tzivanidis, Finite-difference prediction of transient indoor temperature and related correlation based on the building time constant, Int. J. Energy Res. 20 (1996) 507–520.
[18] Y. Wang, L. Wang, W. Hu, P. Sun, Influence of the Heat Transfer Coefficient of the Outer-Surface on the Natural Convective Heat Transfer Characteristics in a Heating Room, vol. 36, 2015, pp. 1206–1211, https://doi.org/10.3969/jheu.201411055.
[19] S. Alfarawi, H. Omar, A. El-Sawi, A. Al Jubori, Thermal performance assessment of external wall construction for energy-efficient buildings, European Journal of Sustainable Development Research 6 (3) (2022), em0189.
[20] P. Bahramnia, S.M. Hosseini Rostami, J. Wang, G-j Kim, Modeling and controlling of temperature and humidity in building heating, ventilating, and air conditioning system using model predictive control, Energies 12 (24) (2019) 4805, https://doi.org/10.3390/en12244805.
[21] Donghun Kim, Wangda Zuo, James Braun, Michael Wetter, Comparisons of building system modeling approaches for control system design, Proceedings of BS 2013: 13th Conference of the International Building Performance Simulation Association (2013), https://doi.org/10.26868/25222708.2013.1409.
[22] P. Riederer, MATLAB/simulink for building and HVAC simulation - state of the art, IBPSA 2005 - International Building Performance Simulation Association (2005).
[23] R. Kramer, J. van Schijndel, H. Schellen, Simplified thermal and hygric building models: a literature review, Frontiers of Architectural Research 1 (4) (2012) 318–325. ISSN 2095-2635.
[24] J. Cockroft, D. Kennedy, M. O'Hara, A. Samuel, P. Strachan, P. Tuohy, Development and Validation of Detailed Building, Plant and Controller Modelling to Demonstrate Interactive Behaviour of System Components, 11th International IBPSA Conference, 2009, pp. 96–103.

[25] D. Testi, E. Schito, E. Tiberi, P. Conti, W. Grassi, Daniele Testi, Eva Schito, Emidio Tiberi, Paolo Conti, Walter Grassi, Building energy simulation by an in-house full transient model for radiant systems coupled to a modulating heat pump, Energy Proc. 78 (2015) 1135–1140. ISSN 1876-6102.
[26] V. Pukhkal, Numerical modeling of energy consumption in residential Buildings4, IOP Conf. Ser. Mater. Sci. Eng. 1079 (2021), 052025.
[27] F. Bre, V.D. Fachinotti, A computational multi-objective optimization method to improve energy efficiency and thermal comfort in dwellings, Energy Build. 154 (2017) 283–294. ISSN 0378-7788.
[28] N. Delgarm, B. Sajadi, S. Delgarm, F. Kowsary, A novel approach for the simulation-based optimization of the buildings energy consumption using NSGA-II: case study in Iran, Energy Build. 127 (2016) 552–560. ISSN 0378-7788.
[29] Y. Lu, S. Wang, Y. Zhao, C. Yan, Renewable energy system optimization of low/zero energy buildings using single-objective and multi-objective optimization methods, Energy Build. 89 (2015) 61–75. ISSN 0378-7788.
[30] W. Yu, B. Li, H. Jia, M. Zhang, D. Wang, Application of multi-objective genetic algorithm to optimize energy efficiency and thermal comfort in building design, Energy Build. 88 (2015) 135–143. ISSN 0378-7788.
[31] Markus Sulzer, Andreas Christen, Andreas Matzarakis, Predicting indoor air temperature and thermal comfort in occupational settings using weather forecasts, indoor sensors, and artificial neural networks, Build. Environ. 234 (2023), 110077. ISSN 0360-1323.
[32] G. Di Ruocco, La riqualificazione della periferia urbana di Salerno tra valorizzazione architettonica e sostenibilità ambientale, CUES, 2010. ISBN: 9788895028699.
[33] A.A. VV, L'architettura INA Casa (1949-1963): Aspetti e problemi di conservazione e recupero, Gangemi Editore, Roma, 2004. ISBN:8849205333.
[34] M.L. Bojic, D.L. Loveday, The influence on building thermal behavior of the insulation/masonry distribution in a three-layered construction, Energy Build. 26 (2) (1997) 153–157. ISSN 0378-7788.
[35] G. Cuccurullo, Elementi di termodinamica e trasmissione del calore, Maggioli editore, 2020. ISBN 8891645289.
[36] M.W. Liddament, A review of ventilation and the quality of ventilation air, Indoor Air 10 (3) (2000) 193–199.